International Journal of Bridge Engineering (IJBE), Vol. 10, No. 3, (2022), pp. 37-62

CRITICAL REVIEW AND MODELLING OF THE CONSTRUCTION SEQUENCE AND LOADING HISTORY OF THE COLLAPSED MORANDI BRIDGE

Andrea Orgnoni[1], Rui Pinho[2], Matteo Moratti[3], Nicola Scattarreggia[1] and Gian Michele Calvi[1]

[1] University School for Advanced Studies, IUSS Pavia, Italy
[2] Department of Civil Engineering and Architecture, University of Pavia, Italy
[3] Studio Calvi Ltd, Pavia, Italy
e-mail: andrea.orgnoni@iusspavia.it, rui.pinho@unipv.it, matteo.moratti@studiocalvi.eu, nicola.scattarreggia@iusspavia.it, gm.calvi@iusspavia.it

ABSTRACT: The Viaduct over the Polcevera River, designed by Riccardo Morandi, was a very strategic and important bridge, built in Genoa (Italy) in the mid-60s. In addition to being a renowned engineering work, due to a very innovative design at that period, the bridge was also considered as one of the symbols of the city. On the 14th of August 2018, however, a portion of this bridge suffered a catastrophic sudden collapse that caused 43 casualties. In order to be able to understand, within the context of the necessary numerical forensic investigations, the stress state to which the bridge was subjected to at the moment of collapse, it is first necessary to reproduce both its construction sequence, as well as the loading history the structure was subjected to throughout its life. This work is thus focussed on such task, as well as on showing the differences between the construction sequence that had been initially envisaged at the design stage and the one that was then actually followed during construction. The analyses carried out highlight how important is the correct modelling of the construction sequence, showing how the use of unknowingly incorrect inputs, may give rise to erroneous stress state estimations, which can then in turn mislead post-collapse forensic studies. In addition, the changes in permanent loading (e.g. addition of asphalt layers, replacement of road barriers) and time-dependent effects (e.g. concrete creep and prestress relaxation) over the course of the 51 years of life of the structure, are also scrutinised and discussed, with a view to try to reproduce as accurately as possible the stress state conditions of the structure at the time of its failure.

KEYWORDS: Polcevera Viaduct; Morandi Bridge; Construction Sequence, Loading History, Time-dependent effects.

1 INTRODUCTION

The so-called Morandi bridge (Figure 1(a)), built in the period 1963-1967, represented, prior to its collapse on 14th of August 2018, an important infrastructure for the Italian road network, part of the motorway connecting several North-West urban centres to the French border (A7 Milano – Genova, A10 Genova – Savona). While the entire structure, as well as its foundation scheme, is comprehensively described in e.g. Morandi [1], in what follows special attention will be given to the "balanced system" that actually collapsed (i.e. balanced system 9), highlighted in Figure 1(b), where the bridge support points are numbered sequentially from the Savona to the Genoa side.

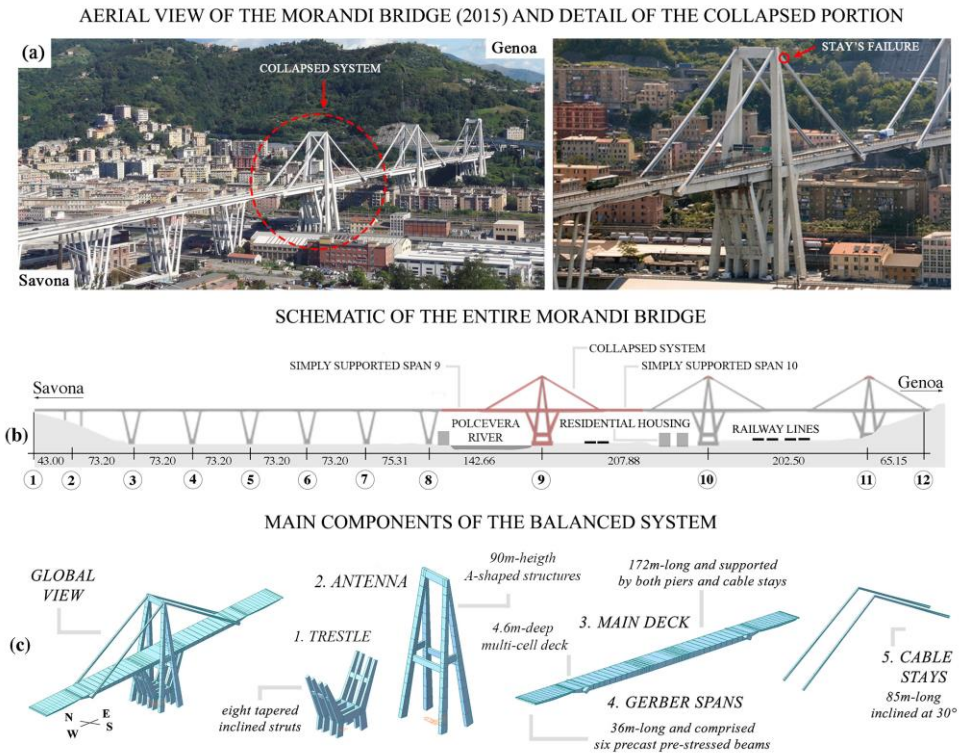

Figure 1. (a) Aerial picture of the bridge (left) and of the collapsed portion (right), (b) schematic of the bridge and (c) main components of the balanced system designed by Morandi.

With reference to the nomenclature reported in Figure 1(c), the considered balanced system comprised the following main elements:

1. A trestle with eight inclined struts (with tapered cross-sections varying between 4.5x1.2 and 2.0x1.2 m) that prop the deck at a height of about 45 m, over a distance of about 40 m.
2. An antenna with two 90.2 m height A-shaped structures (hollow tapered cross-

sections varying between 4.5x0.9 and 2.0x3.0m) that converge at approximately 45 m above the deck level. In addition to the transverse beam at the top of the antenna, four transversal beams (two for each direction) are also present at a height of about 40 m.

3. A main deck with a five-cell box section of predominant height of 4.5 m (it decreases to 1.8 m at its extremities), an upper and lower slabs 16 cm thick, and six deep webs with thickness varying between 18 and 30 cm. In its final configuration, the deck of balanced system 9 was 172 m long and supported at four points: from below by the trestle at the spacing of 40 m, and from above by the cable stays at a distance of 150 m; two 11 m cantilevers completed therefore the deck's length. Four transverse link girders connected stays and trestle struts to deck. Three series of post-compression cables were located along each half of the deck: one across the trestle-deck connection, one between the trestle and the stays connections, and one across the stays' transverse beam. Readers are referred to the work by Scattarreggia et al. (2022) [2] for a more in-depth description and discussion of the deck's characteristics.
4. Two simply-supported 36 m long spans that connect the balanced system to the adjacent parts of the bridge. Each span was made of six precast prestressed beams, with a variable depth from 2.20 m at mid-span to 1.60 m at the extremities, sitting on Gerber saddles protruding from the main deck.
5. Four post-compressed reinforced concrete (RC) cable stays, hanging from the antenna's top and intersecting the deck at an angle of about 30°. Each cable stay is made of 352 ½" high resistance steel strands, encased by a concrete sleeve that is post-compressed by 112 strands of the same type, as depicted in Figure 2.

In the present work, the actual construction sequence of the collapsed balanced system is reproduced, building on the initial work of Orgnoni [3] and using the Midas Civil [4] software. The construction sequence of this bridge was first described by Morandi (1967) [1], and then also discussed by Martinez y Cabrera et al. (1994) [5], Malerba (2014) [6], Calvi et al. (2019) [7], Malomo et al. (2020) [8], Domaneschi et al. (2020) [9] and Morgese et al. (2020) [10]. The work by Morandi (1967) [1], published right after the opening of the viaduct, briefly described the construction sequence of the balanced systems (leaving the impression, it is noted, that such sequence was identical for all three structures); although not many details were included in such construction sequence description, it appeared that the addition of the simply supported spans 9 and 10 (see Figure 1b) took place between the phase that involved the completion of the deck and the beginning of the construction of the stays concrete sleeves.

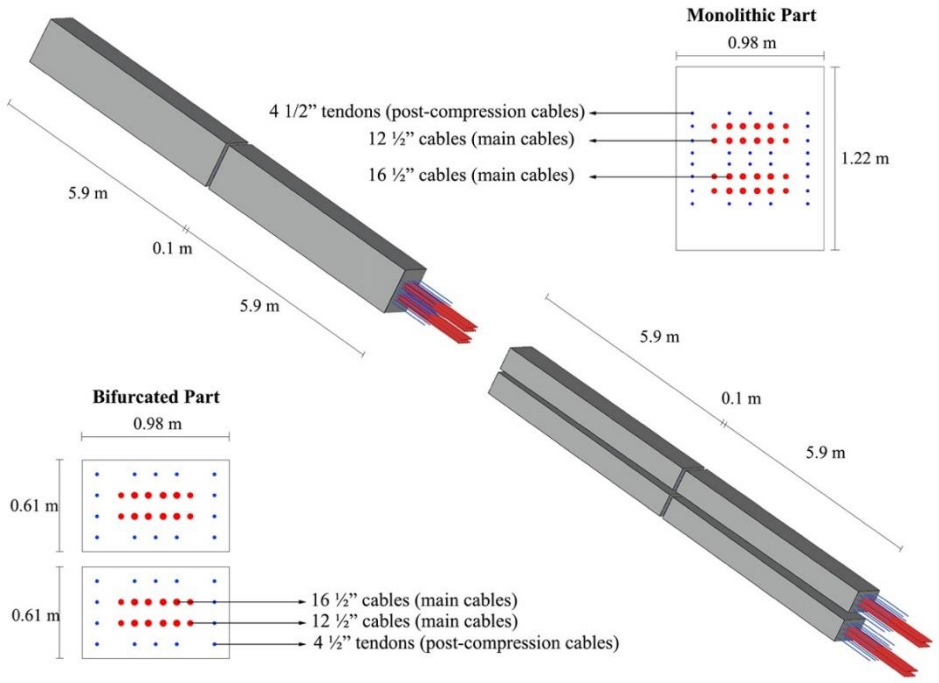

Figure 2. Schematic of a reinforced concrete post-compressed stay

On the contrary, in the work of Martinez y Cabrera et al. (1994) [5], in which the operations for retrofitting the stays of balanced system 11 are described in detail, the construction sequence description indicated that the addition of the deck dead loads, such as road paving and simply supported spans, had instead occurred after the completion of the stays in the balanced systems. Such publication was however referred explicitly to balanced system 11 alone, and did thus not clarify if such construction sequence deviation from the original description of Morandi [1] applied also to the other two balanced systems (9 – 10). The same can be stated for the study presented by Malerba (2014) [6], in which the construction stage relating to the addition of the simply-supported spans is not reported in the text, thus implying as well that the addition of those elements occurred after the completion of the stays. Also, in such publication it was again not explicitly clarified whether the described construction sequence related to a single balanced system or to all three. Many studies carried out subsequently to the collapse of the bridge (e.g. [7-10]) adopt as the construction sequence of the collapsed balanced system (9) that described by Martinez y Cabrera et al. (1994) [5] and Malerba (2014) [6]. This uncertainty on the exact construction sequence of the bridge will be explicitly scrutinised in the present work.

In Section 2 of this paper, the construction sequence described in the original design documentation preserved at the Italian Central State Archives [11], which

is the same as reported by Morandi (1967) [1], is numerically modelled, with the ensuing results being then compared with the structural response estimates found in the original design documentation.

In Section 3, the changes in permanent loading (e.g. addition of asphalt layers, replacement of road barriers) and time-dependent effects (e.g. concrete creep and prestress relaxation) over the course of the 51 years of life of the structure are added to the numerical model. In addition, the temporal sequence with which the stays were constructed is also therein considered.

Finally, Section 4 includes a brief sensitivity study aimed at highlighting how the assumption of construction sequence or execution times described in available design documentation or publications, but different from the actual construction (as evidenced in photos and video footage from that time), can give rise to erroneous stress state estimations at the time of collapse, which may then in turn mislead post-collapse forensic studies.

2 CONSTRUCTION SEQUENCE MODELLING

2.1 Model characteristics

2.1.1 Geometrical configuration

The numerical model is based on the actual geometry of the collapsed structure (balanced system 9, see Figure 1b and Figure 3), as deduced from a 3D survey [12], and which indicated some (relatively minor) deviations in geometry with respect to the initial perfectly symmetric design of the balanced system (Figure 3b), reported in Morandi (1967a) [1]. However, examination of the aforementioned original documents (in particular, drawings n.275 and n.414 [11]) did confirm that the slight skewing detected by the survey at the base of the antenna-trestle structure (Figure 3a) is actually substantially in line with what was reported in the final construction drawings. These geometrical differences concern only the antenna and the trestle (the geometry of the deck and the stays is essentially the same) and the effects on the stress and deformation state appeared to be of little relevance (we ran preliminary analyses considering both configurations). For this reason, reference will always be made in the subsequent sections of this paper to the numerical model that reproduces the actual geometry of the bridge (Figure 3a).

For the sake of completeness, we note also that from the survey it was possible to notice some slight geometric differences between Systems 9 and 10, not the subject of the current work, but discussed in Orgnoni et al (2023) [13].

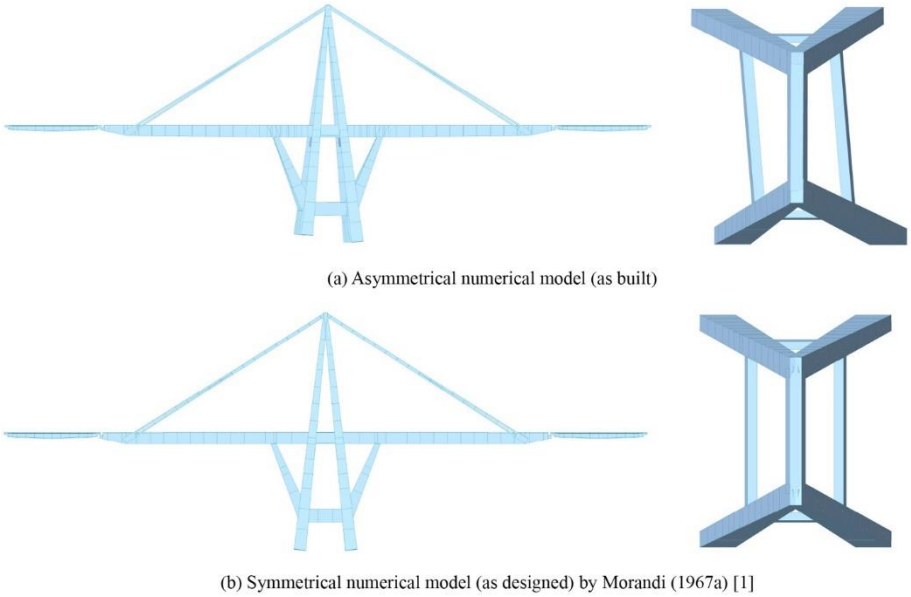

Figure 3. Comparison between Asymmetrical (actual construction) and Symmetrical (original design) configuration (note: the discretization of the deck in model (a) appears different from that of deck (b) because it follows the updated deck reinforcement detailing discussed in [2])

2.1.2 Material properties

The numerical model adopted the values reported in Morandi (1967a) [1], which foresaw the employment of two types of concrete, differing mainly in the dosage of cement. For the non-prestressed structures, such as antenna and trestle, a standard concrete with a dosage of 300/730, to which corresponds a nominal compressive cube strength of 35 MPa, was used, while for prestressed structures (main deck and simply-supported spans) the dosage 350/730, with a nominal compressive cube strength of 48 MPa (high-strength concrete), was adopted. Elastic moduli were assumed to be respectively equal to E = 30 GPa and E = 35 GPa for standard and high strength concrete.

For what concerns instead the deck's tendons, 7 mm diameter wires with tensile strength of 1750 MPa were used, whilst for the prestressing cables of the stays, strands with a nominal diameter of ½ inch were used, also with a tensile strength of 1750 MPa. Elastic modulus and shear modulus of elasticity were assumed to be respectively equal to E = 200 GPa and G = 80 GPa. For the construction of the antenna and the trestle, smooth Aq50 steel bars, with a nominal yield strength of 270 MPa, were employed, while for the construction of prestressed structures, such as the deck and simply supported spans, ribbed bars with yield strength around 440 MPa were considered. It is nonetheless noted that in the numerical model object of this work, the reinforcement was not explicitly implemented, given the linear elastic nature of the analyses undertaken.

2.1.3 Construction sequence overview

As mentioned above, the construction sequence herein considered is based on documents available at the Italian Central State Archive [11], and is in line with what is reported by Morandi (1967a) [1], while it differs from what is reported by other authors [5-10] for what concerns the timing of the installation of the simply-supported spans and the addition of the initial road paving (such differences will be scrutinised and discussed in Section 4 of this paper).

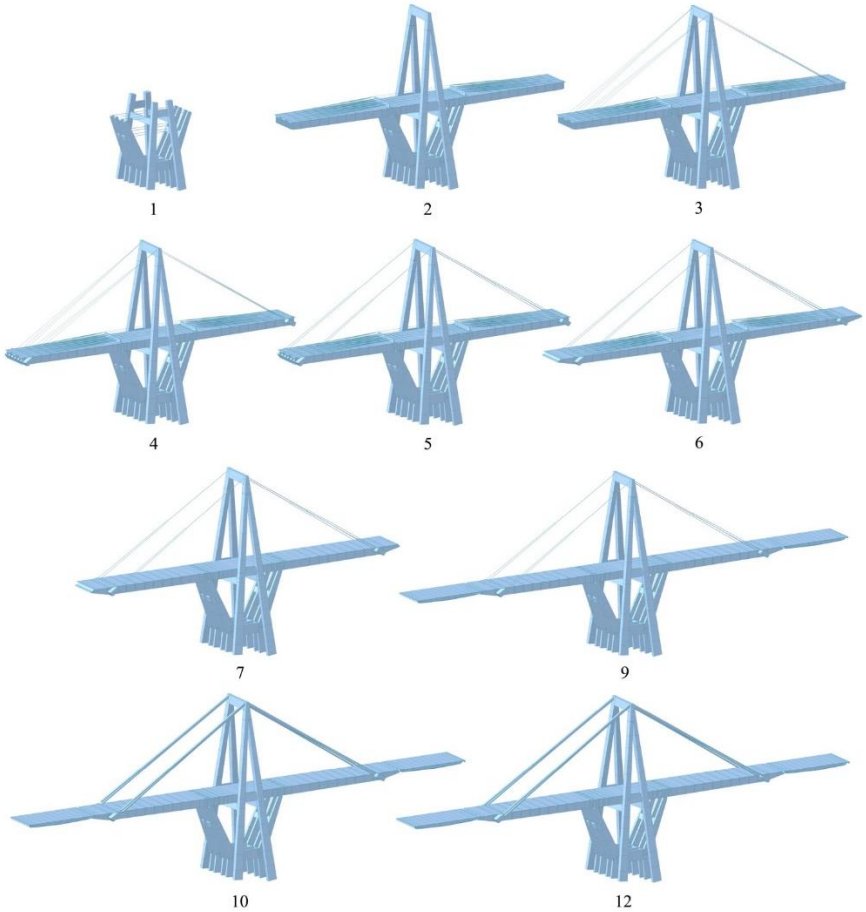

Figure 4. Model screenshots at the end of some of the construction phases defined by Morandi [11]. (note: not all construction stages are herein depicted, since some did not imply a visually perceptible change in the numerical model)

The main construction phases, partially depicted also in Figure 4, are the following:

1. Construction of antenna and trestle (section 2.2.1)
2. Construction of the main deck (section 2.2.2)
3. Installation of the temporary stays (section 2.2.3)

4. Tensioning of the temporary stays and construction of transverse girders (section 2.2.4)
5. Installation of the main cables of the stays and removal of temporary stays (section 2.2.5)
6. Completion of the main deck (cantilevered ends) (section 2.2.6)
7. Removal of temporary deck support cables and completion of its post-compression (section 2.2.7)
8. Removal of deck's movable truss formworks (section 2.2.8)
9. Construction of the simply supported spans (section 2.2.9)
10. Construction of the stays' concrete sleeves (section 0)
11. Addition of deck's dead loads (section 2.2.11)
12. Completion of the stays' concrete sleeves (section 2.2.12)

In the subsequent sub-sections, the construction phases listed above are described in detail, often with the aid of photos from the construction period and screenshots of the numerical model. A discussion on the construction sequence results is then carried out at the end of this Section.

2.2 Detailed description of the construction sequence

2.2.1 Construction of antenna and trestle

The antenna and the lower part of the trestle were built through standard cast-in-place RC construction procedures, such as the use of steel formwork and propping. In the first part of the trestle's construction (M-I-H-L, Figure 5) the bending moments induced by the self-weight of the inclined struts had to be resisted by the elements themselves.

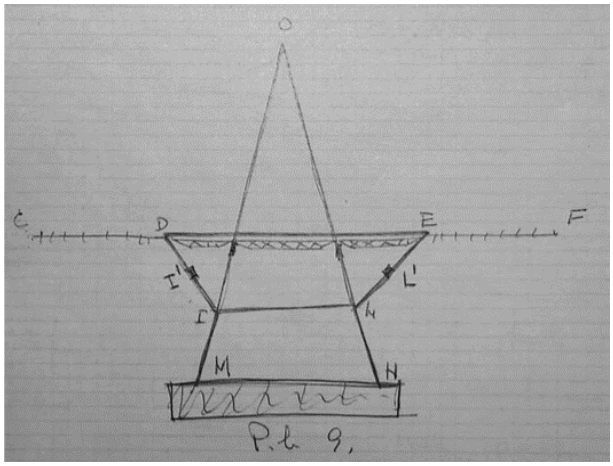

Figure 5. Antenna and trestle original sketch from design documentation [11]

Subsequently, however, the opposite segments (I-I' and L-L') were connected to each other through a first series of steel cables (two strands made of 15 steel wires

of 7 mm diameter) and tensioned at 575 MPa to annul the previous deformations and prevent future ones. After this operation, the trestle construction was completed, as depicted in Figure 6 (I'-D and L'-E elements, Figure 5); also in this case the inclined struts were connected to each other with a second series of steel cables, this time tensioned at 200 MPa.

It is noted that a pre-deformation in the concrete elements, induced by the process just described, was created in order to annul deformations related to the future operations, such as the addition of the deck's steel falsework and the construction of the first part of the main deck. After the casting of the first central portion of the main deck (operation described in the next section), the second series of steel cables were further tensioned at 550 MPa, to sustain the increased loading.

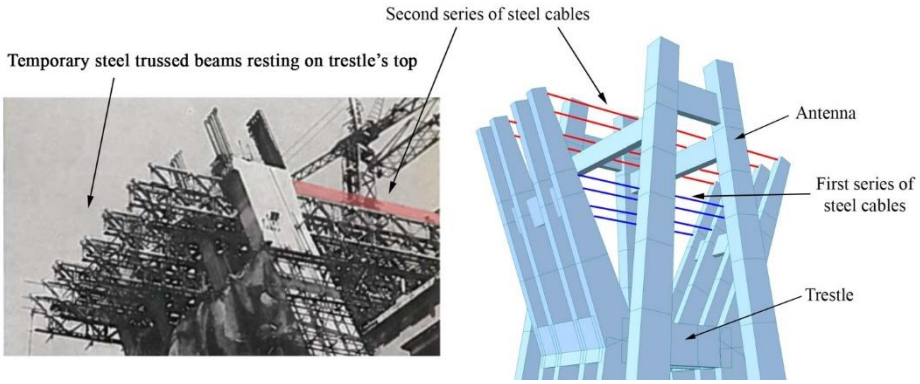

Figure 6. Photo and model rendering of the construction of the trestle and the antenna

2.2.2 Construction of the main deck

The first central portion of the main deck was built between points D and E (Figure 5). The falsework needed for this first deck casting phase consisted of temporary steel trussed beams resting on top of the trestle's struts and the mid-height antenna transversal beams (see Figure 6 and Figure 7). The provisional steel cables, described in the previous section, were removed after the hardening of the concrete in this first portion of the deck, while the steel trussed beams were removed after the construction of two more segments of the deck.

As shown in Figure 7, two steel movable truss formworks were then built to support, for a maximum length of 5.5 m, the segmental concrete casting of the deck, without thus the need to erect from the ground a falsework structure to support the casting. Therefore, the remaining part of the deck was built in the following way:

1. The first segments C11 (Figure 8) and F11 of the deck were built cantilevered, with the help of the movable truss formwork. Subsequently, the tendons inside this deck segments, shown in Figure 9, were tensioned at 900 MPa. The same

procedure was adopted for the following segments, C10 and F10.

2. For the construction of the remaining segments, with length equal to 5.1 m each, a similar construction procedure was employed (use of movable truss formwork), with the difference, however, that a temporary steel cables support system, depicted in Figure 7 and termed "harps" by the designer, was introduced to provide support to the cantilevered deck.

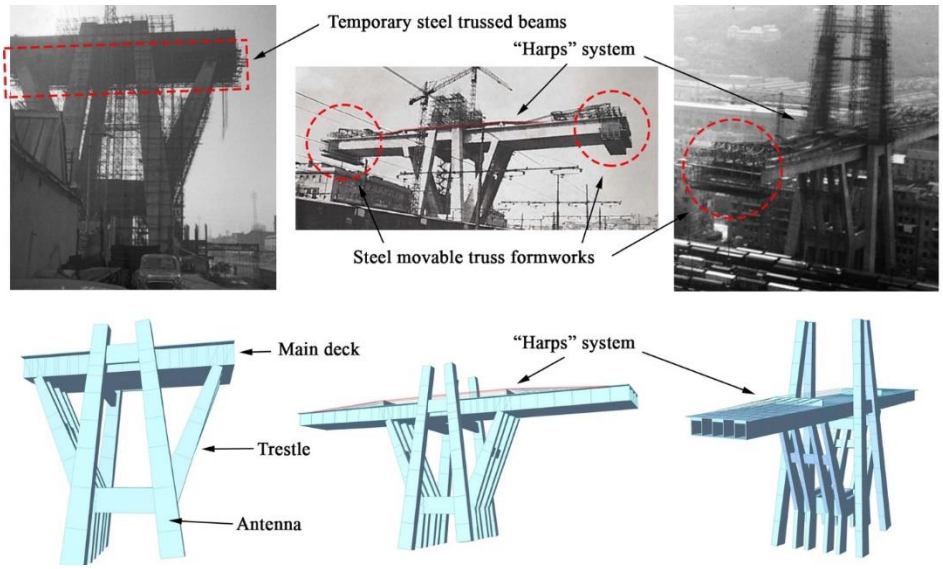

Figure 7. Representation of the main deck's construction technique

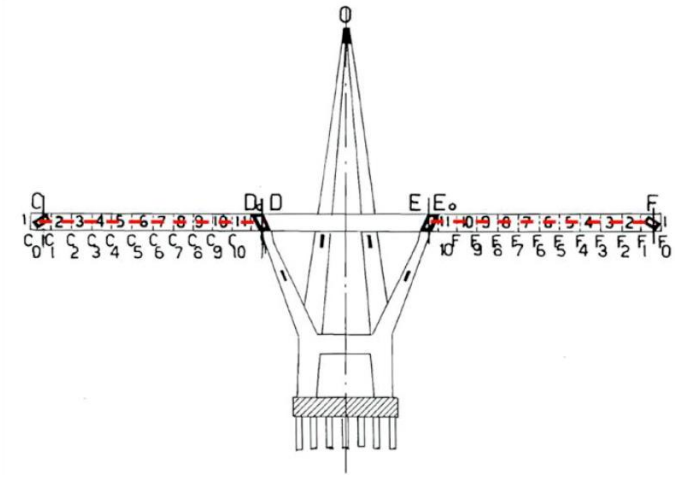

Figure 8. Main deck's segmental casting sequence (starting from segments n.11 and finishing with segments n.0). [12]

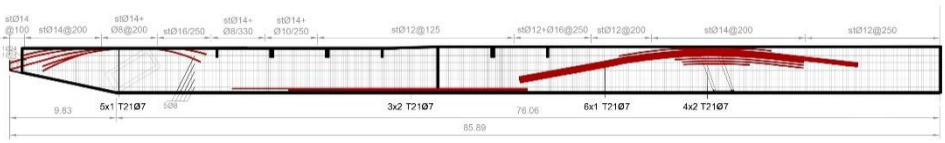

Figure 9. Geometry and reinforcement of a typical internal I-beam portion of the main deck. (Adapted from [8])

The provisional cables constituting the harps system were connected to the upper part of each newly cast deck segment and to the counterpart/symmetrical segment on the opposite side of the trestle, passing over two supports positioned at the centre of the deck (points D and E, Figure 5), at a height of about 2.1 m. Each cable was made of three steel wires of 7 mm diameter (f_y = 1750 MPa) and was tensioned at 920 MPa seven days after the casting of the concrete, for each segment, to allow the compressive strength to reach an acceptable value. From the original drawings, it was possible to observe that the first two segments of the deck built in this way, C09 and C08, were supported by 42 cables made each one by three wires, while the remaining ones, from C07 to C01 (Figure 8), were supported only by 32 cables. In the numerical model (Figure 7), the harps were implemented trough *Cables* elements with an initial stress of 920 MPa, as reported by the designer.

2.2.3 Installation of the temporary stays

After the casting of the final segment of the deck (C01, Figure 8), a set of temporary stays, each of which constituted by 4 cables of 18 ϕ7 steel wires (f_y = 1750 MPa), was installed with a view to provide the necessary support for the casting of the stays transverse girders (Figure 10).

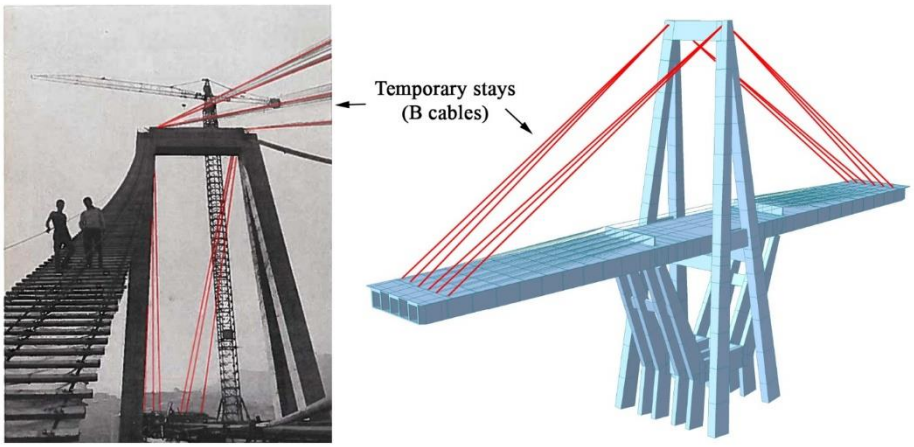

Figure 10. Implementation of the temporary stays

These girders connected the post-compressed RC stays, at this stage yet to be cast, to the main deck. These temporary stays were introduced in the numerical model with a light tensioning of about 55 MPa, as indicated by Morandi [11].

2.2.4 Tensioning of the temporary stays and casting of the transverse girders

This construction stage consisted of three main steps:

1. Tensioning of the temporary stays at 95.5 MPa; in this way, as reported by Morandi [11], the extremities of the deck moved upwards by 230 mm, reaching +45 mm above the deck's level final design target.
2. Cast of the transverse girders: due to the high self-weight of these elements, the control point (set in correspondence of the middle of the girders), moved downwards by 235 mm, reaching the position of -190 mm below the deck's level final design target. The tensile stress in the temporary stays raised up to 390.5 MPa.
3. Tensioning of the post-compression cables (see construction drawing n.314, [11]) inside the transverse girders (it is noted that, in the numerical model, these specific elements were implemented without considering their post-compression cables layout).

2.2.5 Installation of the main cables of the stays and removal of the temporary stays

The main cables of the stays (termed by some as "primary cables") were constituted by 353 ½ inch steel strands, made of high strength steel. They were implemented in the model considering a *Cables* element with an equivalent diameter equal to 0.20 m for the upper part of the post-compressed RC stays, and 0.14 m for each branch of the bifurcated part. This construction stage consisted of two principal steps:

1. The main cables of the stays were installed and initially tensioned at 50 MPa. The control point mentioned above moved upwards by 110 mm (reaching a position of -80 mm below the deck's level final design target). During this operation, the tensile stress in the temporary stays decreased from 391 MPa to 253 MPa.
2. Removal of temporary stays. The tensile stress in the definitive stay cables raised up to 112.7 MPa and the control point position necessarily dropped, to a value that, however, we were not able to find specified in the design documentation (our numerical model estimated a drop of around 55 mm).

2.2.6 Completion of the main deck (cantilevered ends)

This construction stage consisted of two main steps:

1. Casting of the cantilevered ends of the deck, adopting the same procedure used for the previous segments. The tendons inside these sections (Figure 9) were

tensioned at 1050 MPa. Due to the increment of the weight, the stress in the stays' cables raised up to 181.3 MPa and the control point position moved downwards to -190 mm below the deck's level design target.
2. Tensioning of the stays' cables at 200.9 MPa, according to Morandi, raising the control point by 190 mm; at this stage their position was thus at the deck's level design target.

2.2.7 Removal of temporary deck support cables and completion of its post-compression

After the completion of the deck, the temporary deck supporting cables (the "harps") were removed, with the control point consequently lowering to a position of -141 mm below the deck's level design target. At this stage, the deck was sustained at its extremities only by the stays' cables. All the post-compression cables inside the deck (Figure 9) were tensioned.

2.2.8 Removal of deck's movable truss formworks

The movable truss formworks were dismantled at the extremities of the deck and lowered to the ground.

2.2.9 Construction of the simply supported spans

This construction stage consisted of three main steps:
1. Tensioning of the transverse girders' tendons at 1135 MPa.
2. Tensioning of the stays' main cables at 411.6 MPa and consequent raising of the control point to +180 mm above the deck's level final design target.
3. Installation of the simply-supported spans (Figure 11); the control point position would have certainly been lowered (we estimate by around 60 mm), but we were again not able to find Morandi's calculation of this value in the design documentation.

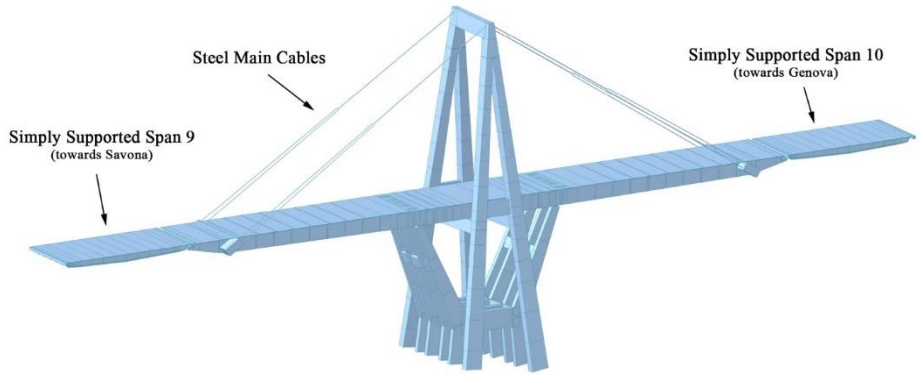

Figure 11. Installation of the simply-supported spans

It is underlined that, differently from what was suggested in [5-6], and, subsequently, adopted also by others [7-10], the simply supported spans of the collapsed balanced system (namely supported spans 9 and 10, Figure 1b) were installed before the casting of the post-compressed concrete sleeve of the stays (i.e. the stays consisted only of their main cables). This is a non-negligible detail, given that if the simply-supported spans had been installed subsequently, rather than prior, to the casting of the stays' concrete sleeves, they would have necessarily induced a counterproductive reduction of the post-compression level.

On the contrary, the application of such dead load before the completion of the RC stays, increases the tensile force in the cables only. In Section 4 of this manuscript, the impact of adoption a different construction sequence (which was actually adopted for balanced system 11) is studied and further discussed.

2.2.10 Construction of the stays' concrete sleeves

This construction stage consisted of two steps:

1. Installation of the prestressing tendons of the stays' concrete sleeves (termed by some as "secondary cables"), needed to post-compress the concrete sleeves after their casting, and consisting of 112 ½" high strength steel strands. They naturally ran parallel to the main cables of the stays, but were introduced in the numerical model as *Tendons* (not as *Cables*).
2. The concrete sleeves (see Figure 12) were built from the deck level up to the top of the antenna, in 5.9 m long segments, separated by a 0.1 m space between each other; this segment spacing is particularly evident in Figure 12b, which refers to a different bridge (Carpineto I viaduct), designed always by Morandi [14], that featured an analogous structural system, albeit using precast concrete sleeve segments. Owing to this construction sequence, the stays (now constituted by the main cables, the not yet tensioned prestressing tendons, and the progressively cast concrete sleeve segments) were free to deform, thus naturally assuming a catenary configuration dictated by their own self weight, without the introduction of bending and shear stresses in the concrete sleeve segments, which are not yet joined through post-compression.

   At the lower extremity, hence close to the deck level, a space of 2 m was let free (see Figure 12a and Figure 13), needed to carry out the post-compression of the concrete sleeves. In Figure 13, the evolvement, as construction progresses, of the deformed shape of the stays up to its final catenary configuration, is depicted.

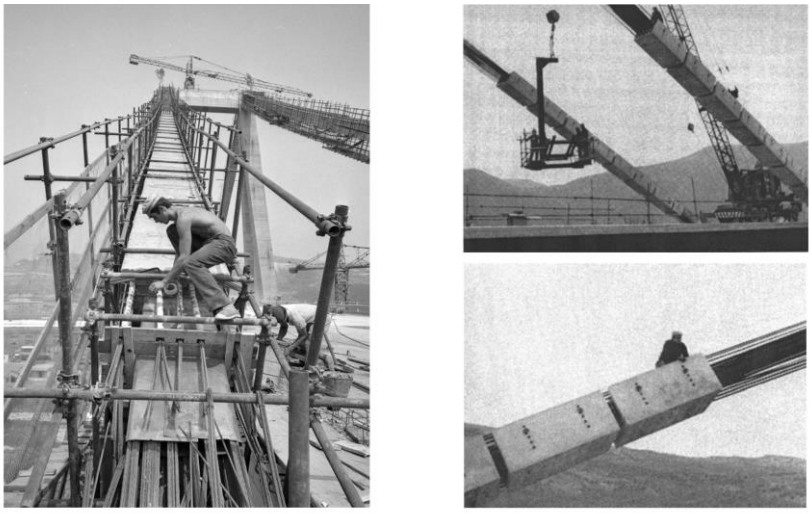

(a) Polcevera Viaduct (b) Carpineto I Viaduct [14]

Figure 12. Construction of post-compressed RC stays: (a) Polcevera viaduct (photo taken in 1967 by De Biasi [15], but publicly circulated, by US newspapers, only subsequently to the collapse of the bridge [16]); (b) Carpineto I Viaduct (contrarily to the case of the Polcevera viaduct, in the Carpineto bridge, designed a decade later also by Morandi, precast concrete sleeve elements were used, installed always from the deck level up to the top of the antenna)

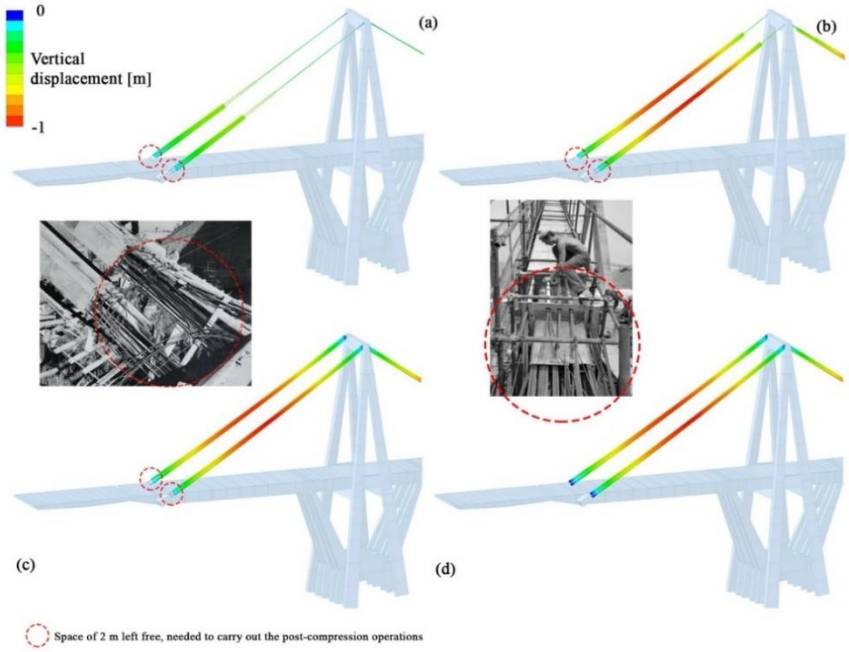

Figure 13. RC stays construction sequence. (a-b) Construction of concrete sleeves from deck level up to top of the antenna. (c-d) completion of the main part of the stays by filling gaps left open and applying post-compression (operation described in section 2.2.12)

2.2.11 Addition of the deck's dead loads

As this construction stage, the road paving was added on top of the 15 m wide bridge deck (it consisted of a 120 mm thick (on average) layer with a 20 kN/m^3 specific weight), along with a number of additional components (see Table 1). These loads caused the tensile stress in the main cables of the stays to raise to a value of 686 MPa and the deck control point to lower down to their envisaged final design target level; it is noted that the resulting variation in the stays' catenary shape did not induce any straining in their concrete sleeves, given that the segments were yet to be joined.

Table 1. Design permanent loads

Load component	Value [kN/m]
Road paving	36
Sidewalk and central curbs	7
Safety rails	1.2
Sidewalks	1.8
Total	**46 kN/m (19% of the deck's dead load)**

2.2.12 Completion of the stays' concrete sleeves

Once all the permanent loads had been applied, and the stays had thus reached their final catenary configuration, the 10 cm gaps between the concrete sleeve segments were closed (through concrete casting), so that the stays could then be post-compressed. This operation involved the tensioning of the prestressing tendons to 686 MPa, the same tensile stress that was at this stage present also in the main cables of the stays. Having both sets of cables tensioned to matching values was part of the so-called "stay homogenisation" strategy envisioned by Morandi, which involved also, as a final step, the injection of the ducts hosting the prestressing tendons. Such injection operation was however only partially completed; pre- and post-collapse inspections revealed the presence of voids inside the ducts (Mortellaro et al. [17], Rosati et al. [12]).

2.3 Comparison between numerical results and original design calculations

In Figure 14 and Figure 15, a comparison between the numerical results and the original design calculations described both in Morandi's design report [11], as well as in the synoptic table of the cable tensioning operations (design table n.366, [11]), is carried out. The comparison regards the values of control point vertical displacement and tensile stress in the main cable of the stays, at each one of the construction phases described in the previous sub-sections, with "CS4.1" standing for Construction Stage number 4 step 1, "CS4.2" standing for Construction Stage number 4 step 2, and so on.

The differences at the completion of the balanced system are minimal, both in terms of vertical displacement at the deck's control point (Δ = 1 mm), as well as with regards the tensile stress in the main cable of the stays (Δ = 21 MPa, i.e. 3% variation). This is a testament to Morandi's structural analysis competence, given that he obtained the above estimates through hand-calculations, rather than through the use of advanced finite element models.

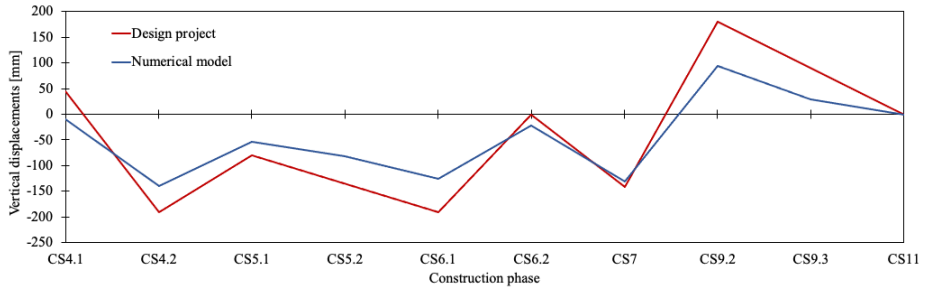

Figure 14. Control point vertical displacement comparison.

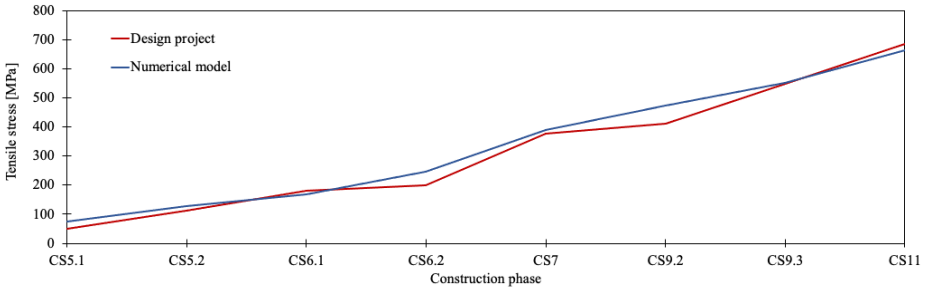

Figure 15. Stay cables tensile stress comparison.

3 DEMAND ON THE RUPTURED SOUTH-EAST STAY, FROM CONSTRUCTION COMPLETION TO COLLAPSE

3.1 Introduction

As shown by Calvi et al. (2019) [7] and Malomo et al. (2020) [8], a sudden rupture at the top end of one of the bridge stays constituted the triggering cause behind the collapse of balanced system 9 of the Polcevera viaduct, a hypothesis that was subsequently confirmed by the public release of video-footage of the event [18]. For this reason, we herein analyse in detail the evolution of axial force, bending moment and residual post-compression in this stay throughout its life. To do so, particular attention was placed on time-dependent effects, such as e.g. relaxation of prestressing tendons or concrete creep, along with the actual execution times for the construction and completion of the post-compressed RC stays, as well as the modifications (e.g. addition of asphalt layers, replacement of road barriers)

carried out on the structure.

3.2 Modelling of time-dependent phenomena

The creep and shrinkage phenomena were modelled in Midas Civil according to CEB-FIP 2010 model code indications [19]. The creep, or viscosity, coefficient (ϕ) is defined as a function of the characteristic compressive strength of the concrete (f_{ck}), the relative humidity of the environment (HR), the ratio between the area of the element and the perimeter exposed to the atmosphere (h_0), the typology of cement used and the age of the concrete at the application of the first load. Shrinkage, on the other hand, depends on the type of concrete used, h_0, and the HR factor. These input parameters were taken from Morandi (1967a) [1] and are summarised in Table 2, whilst the resulting creep and shrinkage relationships are shown in Figure 16.

Table 2. Parameters used for the implementation of shrinkage and creep phenomena

Parameter	Value
Characteristic resistance at 28 days	48 MPa
Environmental relative humidity (HR)	70%
Cement typology	32.5 R, 42.5 N
Exposed cross section/perimeter ratio (h_0)	0.38 monolithic part 0.54 bifurcated part
Age of the concrete at the application of the first load	Multiple

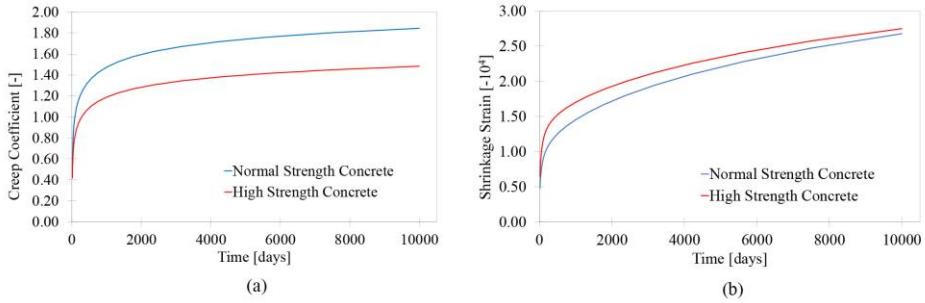

Figure 16. Adopted (a) creep and (b) shrinkage relationships.

For what concerns the prestressing cables, the phenomena of relaxation and tensile force loss due to friction were also simulated. To simulate the relaxation of steel, the model proposed in Eurocode 2 [20] was adopted, whilst the axial force loss due to friction was simulated through the Wobble coefficient, assumed to be 0.0015 m^{-1}, and the Curvature Friction Factor (μ), assumed as equal to 0.3.

3.3 Construction times of the post-compressed RC stays of balanced system 9

From historical archive images [1] it was possible to infer the actual execution times for the construction and completion of the post-compressed RC stays of the three balanced systems of the Polcevera viaduct, and compare such findings with what had been foreseen in the design of Morandi (1967a) [1]. The latter had prescribed an 82 days timeframe for the casting and post-compression of the main portion of the concrete sleeve (i.e. approximately 6 days per segment), followed by a 90 days waiting period before the casting and post-compression of the last segment at the base of the stays (page 32, chapter 14, volume III [11]).

The concrete sleeves of System 9 were, however, actually cast and post-compressed in 23 days only, with the construction of the final closing segment (the one at the bottom of the stay, highlighted in Figure 13c) then starting 6 days after the stay had been cast and post-compressed (note that, for instance, the casting of the stays' concrete sleeves of System 10 was carried out in a 70 days timeframe, much similar to what had been initially envisioned by Morandi). The specific impact on the stress levels of the concrete sleeves brought about by this contraction of the construction times of the stays of System 9 will be scrutinised and discussed in Section 4.2.

Herein, instead, the stress estimates in the stays' concrete yielded by the developed numerical model, considering not only the actual construction schedule, but also the time-dependent effects discussed above, are given, in Table 3, where they are also compared with the values obtained by Morandi in his design calculations. The largest difference, found in the top section of the stay, is of around -11%, possibly associated also to frictional tensile force losses, given that in the original design, and contrary to the present simulation, the frictional head losses were not considered.

Table 3. Post-construction numerical and design compression stresses in the concrete sleeves of System 9

Location	Top [MPa]	Mid [MPa]	Bottom [MPa]
Morandi's design	-6.00	n.d.	-7.20
Numerical simulation	-5.35	-6.29	-7.28

3.4 Maintenance interventions on the bridge

As is common for structures of this type, the Polcevera viaduct was object of a number of maintenance operations during its lifetime [12]. The most noticeable interventions carried out over a period of 14 years from 1990 onwards, concerned the:

- substitution of the original steel guardrails with New Jersey barriers (featuring an estimated weight of 8.75 kN/m and 10.5 kN/m, respectively for the external and central lanes);

- enlargement and strengthening of the sidewalks, which had to sustain the now larger road barriers, and thus became heavier by a 15 kN/m amount;
- retrofitting of some of the precast beams of the simply supported spans (three beams were jacketed in the span towards Savona, and two in the span towards Genoa), which led to an estimated weight increase of 1.3 kN/m per retrofitted beam;
- replacement of the additional non-embedded post-compression cables that had been installed around 1980 in the bottom central part of the caisson deck of the span towards Savona [12], with new Dyform-type strands, always non-embedded in the deck and anchored only at their ends, but now installed both in the part of the deck towards Savona, as well as in that towards Genoa [12].

Although these interventions were, as mentioned above, carried out over a period of 14 years, in the numerical model, and for simplicity, they were considered as being introduced in 1990. It is noted also that the interventions described in the fourth bullet point above could not be implemented in the numerical model, due to a lack of the necessary details, discussed also in [12]. Such modelling absence, however, is not expected to have a significant impact in the results, given the localised nature of the compression forces introduced by these external cables, aimed at reclosing cracking observed at the bottom of the caisson deck.

Again as customary in road infrastructures, over the years various re-asphalting operations took place, and these led to an increase, with respect to the original 120 mm value, of approximately 50 mm in the paving thickness on the main deck of System 9 (and of 20 and 100 mm in the simply supported West and East spans, respectively), as gathered from the examination of the post-collapse remains of the bridge [12]. Once more, and always for the sake of modelling simplification, this increase in paving thickness was applied in a single moment in time, in 2010.

The cumulative variation in non-structural permanent loading induced by the bridge maintenance operations discussed above is non-negligible; when the construction of the bridge was completed in 1967, the ratio between such loading and the self-weight of the main deck's caisson structure was around 19%, whilst in 2010 it had increased to a value of approximately 40%. An identical trend was logically observed also for the simply supported spans, albeit with higher ratios, given the lighter nature of the deck structural systems for such spans.

3.5 Evolution of internal forces demand in the stay

The modifications to which the structure was subjected during its life, discussed previously, caused an increase in the axial force acting in the stays by 17%, as reported in Table 4 (where also the changes in the bending moment acting in the upper part of the South-East stay of System 9 is shown). This led to the variations summarised in Table 5 of axial stress at different locations (top, mid, bottom) of the stay, as derived from the developed numerical model, which, it is recalled,

considered also the time effects on materials (creep, shrinkage, relaxation).

In 1990, before the maintenance interventions were carried out, the value of compressive stress at the section's centroid was about half of that in 1967, decreasing even further after the 1990 interventions. In addition, the increase in the bending moment at the top of the stay, from an almost negligible value at the opening of the bridge (91 kNm) to a value almost 10 times larger at the moment of collapse (850 kNm), would also have induced a reduction of the average state of compression in the upper part of the stay. This could have been exacerbated further by potential differential thermal variations along the stay's section [21], as well as due to the construction defects identified in the post-collapse forensic analysis of the bridge remains [12].

Table 4. Variation of values of axial force and bending moment (at the top of the South-East stay) during the life of System 9

Period during life of structure	Axial force [kN]	Bending moment [kNm]
1967, Opening of the bridge	21749	91
1990, Pre-renovation works	22435	-484
1990, Post-renovation works	24217	462
2010, Pre-reasphalting operations	24442	383
2010, Post-reasphalting operations	25411	884
2018, Pre-collapse situation	25437	850

Table 5. Prestress variation, at the section's centroid, throughout the life of System 9 (- compression stress)

Year	Top of the stay [MPa]	Mid of the stay [MPa]	Bottom of the stay [MPa]
1967	-5.35	-6.29	-7.28
1990 pre-maintenance	-2.83	-3.74	-4.6
1990 post-maintenance	-1.53	-2.44	-3.25
2010 pre-reasphalting	-1.27	-2.16	-3
2010 post-reasphalting	-0.56	-1.45	-2.25
2018	-0.53	-1.42	-2.23
Prestress loss	**90%**	**77.42%**	**69.36%**

4 THE IMPACT OF CONSTRUCTION TIME AND SEQUENCE ASSUMPTIONS

4.1 Effect of a different construction sequence on the stays' stress state

Available documentation, such as Figure 17, shows the construction phases of the viaduct, from the starting of the construction in 1963 to its completion in 1967, revealing that the three balanced systems were not built following the same

construction sequence (further confirmation can also be found in archive video footage available online [22]). In particular, it can be noticed that in balanced system number 9 (Figure 18a) the simply supported spans were added before the completion of the RC stays concrete sleeves (as prescribed by Morandi and assumed in all analyses above), whilst in balanced system number 11 (Figure 18b), the concrete stays were already completed when the simply supported span were to be added, as reported by [5-6].

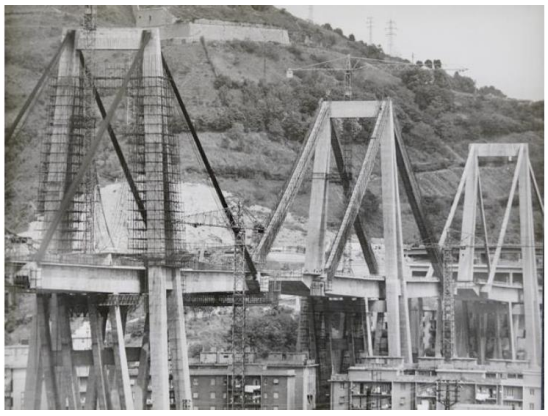

Figure 17. View of the three balanced systems during the installation of the simply supported spans. From left to right: Balanced system 9, 10 and 11. [12]

(a) Balanced System 9 (b) Balanced System 11

Figure 18. Construction sequence differences between balanced system 9 and 11 (frame from [22])

As may be readily gathered from Figure 19, the different construction sequence of balanced system 11 had an important impact in the stress-strain state of its stays; more than half of their length was under tension at the section's centroid, whilst the stays of system 9 were fully compressed (always at the section's centroid). It is thus not surprising that balanced system 11 was, in the early 90's, deemed as needing an urgent retrofitting operation, which was then duly carried out, as described in e.g. Camomilla et al. [23].

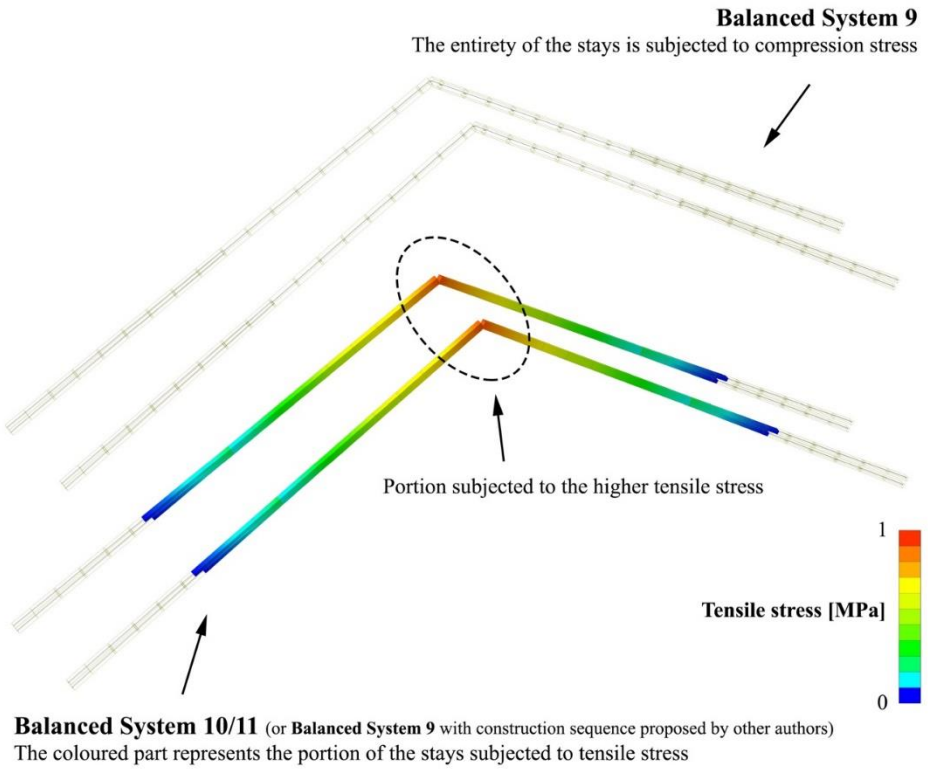

Figure 19. Decompressed portion in balanced system 9 and 10/11 in 1990

4.2 Effects of the execution times on the stay's stress state

As discussed in Section 3.3, the construction times of the stays of System 9 deviated significantly from what had been initially envisaged by Morandi (1967a) [1]. Herein we explore in detail the consequences that such construction times variation had on the stress state of the stays, using the year of 1990 (pre-renovation works) as reference, and adopting also the viscosity coefficients used by Morandi in his original design (Table 6).

Table 6. System 9 stays' creep coefficients, according to design execution times, calculated at t = 10000 days

Segment number	h_0 [m]	t_0 [days]	ϕ
Bifurcated segments	0.38	120	1.008
Monolithic segments	0.54	120	0.97

The results obtained are summarised in Table 7, which do show that, as expected, the accelerated actual construction times of the stays of System 9 caused

compression losses higher than those foreseen in the design. The residual compression differences are of the order of 0.63 MPa (12% of the initial compression) for the upper part of the stays, of 0.57 MPa (9% of the initial compression) for the middle section, and 0.54 MPa (7% of the initial compression) for the lower part. These construction times-induced variations were thus of a relatively minor nature, though they would have contributed to a reduction of the average state of compression in the stays.

Table 7. Prestress losses from 1967 to 1990 (pre-maintenance), considering design and actual construction times (- compression stress)

System – 1990 pre-maintenance	**Top [MPa]**	**Mid [MPa]**	**Bottom [MPa]**
System 9 – actual times	-2.83	-3.74	-4.6
System 9 – design times	-3.46	-4.31	-5.14
Absolute Difference (Design vs Actual)	**-0.63**	**-0.57**	**-0.54**
Relative difference (Design vs Actual)	**-18%**	**-13%**	**-10%**

5 CONCLUSIONS

In this work, a numerical modelling of the collapsed Morandi Bridge was carried out, with a view to study the evolution, during the construction and in the subsequent 51 years of life of the bridge, of the stress-strain state on its failed concrete stay, and be thus able to estimate the force demand to which such stay was subjected to on the day of the collapse.

To start with, a detailed numerical reproduction of the construction sequence of the bridge was carried out. The modest differences observed between the results obtained in this modelling phase, using advanced finite element models, and those attained by Morandi, using only hand-calculations, not only confirm the correctness of the design calculations, but highlight also the structural analysis competence of this designer, especially considering how much less advanced was knowledge on prestressing issues back in the 60's.

Through the execution of a viscoelastic analysis, it was then possible to simulate the effects of time, from the bridge opening in 1967 to its collapse in 2018, on the resistance and deformation of the concrete and steel materials, as well as the influence of the added loads in the various phases of the life of the structure. The addition of the permanent loads related to maintenance operations in 1990, as well as those related to the multiple re-asphalting that occurred over the years, caused, in particular in the South-East stay of the balanced system 9, an increase of about 17% of the axial force present in the stays at the time of opening in 1967. Further, time effects on the materials, coupled with the aforementioned increase in permanent loads throughout the 51 years of life of the

bridge, led to an approximately ten-fold increment of the bending moment at the top of the stay under consideration, compared to the value present in the 1967.

This non-negligible increase in time of flexural internal actions at the top of the stay, which would have been further amplified by traffic loads and potential differential thermal effects [21], and which were seemingly not foreseen at the bridge design stages, certainly contributed to a reduction of the average state of compression in the upper part of this structural element.

The analysis of historical documentation made it also possible to verify how the collapse balanced system 9 was built following a construction sequence different from systems 10 and 11; the latter had permanent finishing loads and the simply supported spans applied after the completion of the post-compressed RC stays, while in the case of system 9 the same loads were added before the stays completion, when only their main cables were operational. The two different construction sequences yielded very different values of residual prestress in the stays, highlighting the importance of an accurate and detailed modelling of all stages of construction for this type of structures, especially in the framework of post-collapse forensic investigations.

The stress states obtained in the time-dependent analyses discussed in this work have served as a starting point for additional investigations aimed at the estimation of the ultimate capacity of the stays at the time of collapse [21] and at the explicit simulation of the bridge's collapse mechanism [2][24]. In addition, a study aimed at exploring the feasibility of in-situ dynamic characterisation endeavours, carried out throughout the years prior to the collapse, being capable of providing an insight on the reduction of the average state of compression in the stays, was also undertaken building up on the results obtained herein [13].

In closing, it is underlined that the modelling work herein described was facilitated by the extensive details and evidence that has now become available through the ongoing post-collapse court proceedings (e.g. [12]).

REFERENCES

[1] Morandi R. (1967a). Il viadotto sul Polcevera per l'autostrada Genova-Savona. L'Industria Italiana del Cemento, XXXVII, 849-872, 1967, (in Italian).

[2] Scattarreggia N., Galik W., Calvi P.M., Moratti M., Orgnoni A., Pinho R. (2022). "Analytical and numerical analysis of the torsional response of the multi-cell deck of a collapsed cable-stayed bridge", Engineering Structures, 265: 114412.

[3] Orgnoni A. (2019). "Critical review and modelling of the construction sequence of the Polcevera Viaduct", Undergraduate Thesis, University of Pavia.

[4] MIDAS IT (2020). Midas Civil – Integrated Solution System for Bridge and Civil Engineering. Available at http://www.midasuser.com

[5] Martinez y Cabrera F., Camomilla G., Donferri Mitelli M., Pisani F. and Marioni A. (1994). "Il risanamento degli stralli del viadotto Polcevera". (in Italian).

[6] Malerba P. G. (2014). Inspecting and repairing old bridges: Experiences and lessons. Structure and Infrastructure Engineering, 10(4), 443-470.

[7] Calvi G.M., Moratti M., O'Reilly G.J., Scattarreggia N., Monteiro R., Malomo D., Calvi P.M. and Pinho R. (2019). Once upon a time in Italy: The tale of the Morandi bridge. Structural

Engineering International, Vol. 29, No. 2, pp. 198–217.
[8] Malomo, D., Scattarreggia, N., Orgnoni, A., Pinho, R., Moratti, M., & Calvi, G. M. (2020). Numerical study on the collapse of the Morandi bridge. Journal of performance of constructed facilities, 34(4), 04020044.
[9] Domaneschi M., Pellecchia C., De Iuliis E., Cimellaro G. P., Morgese M., Khalil A. A., & Ansari F. (2020). Collapse analysis of the Polcevera viaduct by the applied element method. Engineering Structures, 214, 110659.
[10] Morgese M., Ansari F., Domaneschi M., & Cimellaro G. P. (2020). Post-collapse analysis of Morandi's Polcevera viaduct in Genoa Italy. Journal of Civil Structural Health Monitoring, 10(1), 69-85.
[11] Morandi R. (1967b). Documents from Morandi's Archive. Central Archive of the State, Rome, Italy.
[12] Rosati G., Losa M., Valenitini R., Tubaro S. (2020). Perizia. Secondo Incidente Probatorio, Procedimento Penale 27 N. 7998/18 R.G.G.I.P. (N.10468/18 R.G.N.R.). Tribunale Ordinario di Genova, Genoa, Italy.
[13] Orgnoni A., Pinho R., Calvi G.M., Moratti M., Scattarreggia N. (2023). Numerical dynamic characterisation of concrete bridge stays. Earthquake Engineering & Structural Dynamics, submitted.
[14] Della Sala L., Sabatiello A. (2016). Viadotto strallato Carpineto I. Structural Modeling 15, pp 2-13, 2016 (in italian).
[15] De Biasi M. (1967). *Archivio Mario De Biasi*, Mondadori Portfolio, via Getty Images.
[16] Iori T., Poretti S. (2020). *Storia dell'ingegneria strutturale in Italia*. SIXXI vol. 5. 2020.
[17] Mortellaro A. P., Ieovella G., Lombardo F., Nuti C., Vanzi I. (2018). "Relazione commissione ispettiva MIT sul crollo del Viadotto Polcevera", disponibile da: http://www.mit.gov.it/comunicazione/news/ponte-crollo-ponte-morandi-commissione-ispettiva-genova/ponte-morandi-online-la (in Italian).
[18] la Repubblica Ponte Morandi, Le Immagini Inedite Della Tragedia: Il Crollo Ripreso Dalla Videosorveglianza - YouTube Available online: https://www.youtube.com/watch?v=a-LfXohbn0U&ab_channel=LaRepubblica (accessed on 2 September 2021).
[19] CEB-FIP (2010). Fib Model Code for Concrete Structures.
[20] CEN (2004). Eurocode 2: - Design of concrete structures – Part 1-1: General rules and rules for buildings. European Committee for Standardization, Brussels, Belgium.
[21] Pinho R., Scattarreggia N., Orgnoni A., Lenzo S.G., Grecchi G., Moratti M., Calvi G.M. (2023). "Forensic estimation of the residual capacity and imposed demand on a ruptured concrete bridge stay at the time of collapse". Structures, submitted.
[22] Licandro A. (2018). "Immagini storiche della costruzione del Ponte Morandi: il cantiere dal 1963 al 1967", disponibile da: https://www.ilfattoquotidiano.it/2018/08/14/genova-le-immagini-storiche-della-costruzione-del-ponte-morandi-il-cantiere-dal-1963-al-1967/4559908/
[23] Camomilla G., Pisani F., Martinez y Cabrera F. and Marioni A. (1995). "Repair of the stay cables of the Polcevera viaduct in Genova, Italy", IABSE reports.
[24] Scattarreggia N., Orgnoni A., Pinho R., Moratti M., Calvi G.M. (2023). "Numerical modelling of the impact of a falling object on a bridge deck", Engineering Failure Analysis, submitted.